Compressed-Sensing Accelerated 3-Dimensional Magnetic Resonance Cholangiopancreatography
Application in Suspected Pancreatic Diseases

Liang Zhu, MD, Xi Wu, MD,† Zhaoyong Sun, MM,* Zhengyu Jin, MD,* Elisabeth Weiland, PhD,‡ Esther Raithel, PhD,‡ Tianyi Qian, PhD,§ and Huadan Xue, MD**

Objectives: The aims of this study were to prospectively evaluate image quality, duct visibility, and diagnostic performance in duct-related pathologies of compressed-sensing (CS) accelerated 3-dimensional (3D) magnetic resonance cholangiopancreatography (MRCP) prototype protocols and compare these with those of conventional 3D MRCP protocol in patients with suspected pancreatic diseases.

Material and Methods: The institutional review board approved this prospective study and all patients provided written informed consent. A total of 80 patients (47 men and 33 women; median age, 57 years; age range, 24–87 years) underwent 3D MRCP at 3.0 T. Three protocols were performed in each patient in random order: CS breath-hold (BH) protocol, CS navigator-triggered (NT) protocol, and conventional NT protocol. The acquisition time of each protocol was recorded. Image quality and duct visibility were independently rated in random order on a 5-point scale by 2 radiologists, who were blinded to the protocols. Receiver operating characteristic curves were generated, and area under the curve (A_z value) was used to compare the diagnostic performance of each protocol in duct-related pathologies.

Results: Acquisition time was 17 seconds for the CS-BH and 134.1 ± 33.5 seconds for the CS-NT protocol, both being significantly shorter than the conventional NT protocol (364.7 ± 78.4 seconds; both $P < 0.01$). The CS-BH MRCP protocol showed significantly less artifacts compared with the CS-NT and conventional NT protocols (both $P < 0.01$). Visualization of bile ducts was comparable in all 3 protocols, whereas CS-NT and conventional NT MRCP depicted pancreatic duct better than CS-BH MRCP did (for proximal, middle, and distal segment; all $P < 0.05$). Compressed-sensing-NT MRCP had the highest diagnostic performance for detecting ductal anomalies, long-segment duct stenosis, abnormal branch ducts, and communication between cystic lesion and pancreatic duct (mean A_z value, 0.943–0.983).

Conclusions: Compressed-sensing MRCP is feasible in patients with suspected pancreatic diseases. Compressed-sensing-NT MRCP demonstrated superior diagnostic accuracy for duct-related pathologies.

Key Words: compressed sensing, breath-hold, navigator-triggered, magnetic resonance cholangiopancreatography, pancreatic disease

(*Invest Radiol* 2017;53: 150–157)

Magnetic resonance cholangiopancreatography (MRCP) is a well-established imaging technique that allows for noninvasive evaluation of anatomy and pathologies of the pancreaticobiliary system.[1–4] Currently, several techniques are used to obtain MRCP images, including 2-dimensional (2D) breath-hold (BH) thin-section acquisition, 2D BH thick-slab acquisition, and 3-dimensional (3D) isotropic image acquisition with navigator-triggering. The advantage of 3D MRCP over the 2D protocol is that the isotropic/near-isotropic acquisition allows postprocessing reconstruction, which enables observation in unlimited projection views. The major limitation of 3D MRCP is the prolonged imaging time, which usually needs to be obtained with respiratory or navigator triggering, taking several minutes.[5] As a result, 3D MRCP tends to be prone to motion artifacts, especially for patients with irregular breathing patterns. Many efforts have been made to reduce the acquisition time of 3D MRCP, including parallel acquisition or application of other fast sequences.[5–8] Recently, compressed-sensing (CS) has been applied for accelerated magnetic resonance (MR) acquisition, by the means of k-space undersampling and nonlinear optimized iterative reconstruction.[9–14] There have been several pilot studies that investigated the feasibility of CS accelerated 3D MRCP in clinical patients with pancreaticobiliary diseases, adopting either BH protocol or navigator-triggered (NT) protocol.[15,16] These initial results demonstrated comparable image quality and reduced acquisition time compared with conventional protocols. Pancreatic diseases were not specified, and only a few cases were included in these studies though. One recent study compared CS MRCP with conventional 3D MRCP and evaluated the diagnostic performance of both.[17] However, only a small subgroup of the study had pancreatic diseases, and in most of their cases, only CS-NT MRCP was performed. Therefore, the purposes of this study were to investigate the image quality and duct visibility with both CS-BH MRCP and CS-NT MRCP in a larger group of clinical patients with suspected pancreatic diseases and to evaluate the diagnostic performance of CS-MRCP in pancreatic duct–related pathologies.

MATERIALS AND METHODS

Patients

This prospective study was approved by the institutional review board, and all patients provided written informed consent. From October 2016 to May 2017, patients with suspected pancreatic diseases who were scheduled for MRCP examinations were prospectively enrolled. Patients came from our weekly multiple disciplinary clinical team clinic for pancreatic diseases. Inclusion criteria were (1) adult patient (≥18 years old) requiring MRCP for known or suspected pancreatic disease by clinical or previous imaging assessment, (2) no history of pancreaticobiliary surgery, (3) no contraindication for MR study. For patients who received several consecutive MRCP studies (ie, baseline and follow-up studies), only the baseline examination before treatment was taken for evaluation. Patients were excluded if they refused to participate in the study (n = 3), were unable to follow the BH instructions (n = 2, patients had severe hearing impairment), or fail to complete the whole scan with full protocols (n = 1, patient had peripheral nerve stimulation through other sequences during the examination, and only a simplified protocol was performed).

The final patient cohort was composed of 80 patients (47 men and 33 women; median age, 57 years; age range, 24–87 years). Patients'

Received for publication July 24, 2017; and accepted for publication, after revision, August 27, 2017.

From the Departments of *Radiology and †Gastroenterology, Peking Union Medical College Hospital, Beijing, China; ‡Siemens Healthcare Gmbh, Erlangen, Germany; and §MR collaborations NE Asia, Siemens Healthcare, Beijing, China.

Liang Zhu and Xi Wu contributed equally to this work.

Conflicts of interest and source of funding: H. Xue has received funding from the National Natural Science Foundation of China (General Program, no. 81371608) and Z. Jin has received funding from the Health Industry Special Scientific Research Project (no. 201402019). E. Weiland, E. Raithel, and T. Qian are employees of Siemens Healthcare. All other authors declare no conflicts of interest.

Correspondence to: Zhengyu Jin, MD, Department of Radiology, Peking Union Medical College Hospital, Shuaifuyuan No. 1, Dongcheng District, Beijing, China, 100730. E-mail: jin_zhengyu@163.com.

ISSN: 0020-9996/18/5303–0150
DOI: 10.1097/RLI.0000000000000421

indications for the MRCP studies were as follows: cystic pancreatic lesion (n = 29), suspected pancreatic duct anomalies (n = 12), chronic pancreatitis (n = 7), suspected or diagnosed autoimmune pancreatitis (n = 27), groove pancreatitis (n = 1), and candidates for parenchyma-preserving pancreatic tumor enucleation (n = 4).

MR Examination

Magnetic resonance imaging examinations were performed on a 3.0 T MR scanner (MAGNETOM Skyra; Siemens Healthcare, Erlangen, Germany). An 18-channel body array coil and a 32-channel spine coil were used in combination for signal reception. Patients fasted for at least 4 hours before the examination. No spasmolytic drug was administered. Isotropic 3D MRCP was performed using sampling perfection with application optimized contrast using different flip angle evolutions (SPACE) acquisition. Three protocols were performed on each patient: conventional NT prospective acquisition correction (PACE) protocol (conventional NT protocol), CS accelerated NT PACE protocol (CS-NT protocol), and CS accelerated BH protocol (CS-BH-protocol). Compressed-sensing-NT and CS-BH MRCP were measured with a prototype sequence, which applies a sparse, incoherent undersampling scheme using a Poisson-Disk pattern.[15] An acceleration factor of 22 (4.5% k-space data sampling) and 24 (4.2% k-space data sampling) was achieved for the CS-NT and CS-BH MRCP protocol, respectively. The order of the 3 protocols was randomized. When consecutive patients were prospectively recruited, each patient was allocated with a randomized order. Detailed acquisition parameters of the 3 protocols were as follows.

Conventional NT protocol: field of view (FOV): 384–400 × 384–400 mm^2 (adjusted to patient size); repetition time (TR)/echo time (TE), 2400/700 milliseconds; flip angle (FA), 100°; parallel imaging acceleration factor, 3; spectrally selective fat saturation applied; matrix, 384 × 384; section thickness, 1 mm; spatial resolution, 1 × 1 × 1 mm^3; number of coronal sections, 64; averages, 1.7.

CS-NT protocol: FOV: 384 × 384 mm^2; TR/TE, 2400/700 milliseconds; FA 100°; parallel imaging acceleration factor, 3; spectrally selective fat saturation applied; matrix, 384 × 384; section thickness, 1.0 mm; spatial resolution, 1 × 1 × 1 mm^3; number of coronal sections, 96; averages, 1.9.

CS-BH protocol: FOV: 384 × 384 mm^2; TR/TE, 1700/425 milliseconds; FA, 95°; parallel imaging acceleration factor, 3; spectrally selective fat saturation applied; matrix, 384 × 384; section thickness, 1.0 mm; spatial resolution, 1 × 1 × 1 mm^3; number of coronal sections, 64; averages, 1.4.

The CS reconstruction technique used a regularization parameter of 0.002 and 20 iterations.[15,17,18] The inline image reconstruction took approximately 6 minutes for each data set.

The acquisition times of each protocol were recorded separately. Because the CS-NT protocol was set to acquire 96 sections while the other 2 protocols acquired 64 sections, the acquisition time of CS-NT protocol was adjusted in latter comparisons. The CS-NT protocol could have a higher number of sections because it was less restricted by the patient's BH capacity and does not bring much burden to the entire examination time. An experienced technician reconstructed maximum-intensity-projection (MIP) images from source isotropic images of each protocol using a commercial post-processing workstation (Syngo MMWP, VE36A; Siemens Healthcare). Twelve MIP images rotating around the body axis were built routinely for evaluation. Additional free-rotated images were generated whenever necessary, based on the presence of the individual patients' pathology.

Image Analysis

Image Quality Assessment

Two radiologists (with 14 and 5 years of clinical experience in abdominal MR imaging, respectively) independently evaluated the MRCP images. Rotating MIP images were used for evaluation, without referring to the 1 mm originally acquired data. The radiologists were blinded to patient information, acquisition methods, and imaging parameters during image interpretation. No data from other sequences of the clinical examination were made available to the readers. The 3 sets of MRCP images of each patient were randomized, and each set was evaluated with 2 weeks' interval, to minimize recall bias.

The degree of image quality degradation by artifacts was graded on a 5-point Likert-type scale (1 = nondiagnostic image due to severe artifacts, 2 = major artifacts causing significant problem in diagnosis, 3 = moderate artifacts with some uncertainty in diagnosis, 4 = minor artifacts without problems in diagnosis, 5 = excellent image quality without any detactable artifacts). Background suppression was also graded on a 5-point scale (1 = significant background signal that rendered image interpretation impossible, 2 = remarkable background signal that rendered image interpretation difficult, 3 = noticeable background signal that is distracting in image interpretation, 4 = minimal background signal without problems in observation of pancreaticobiliary tree, 5 = excellent background suppression).

The readers also evaluated visualization of 7 segments of the pancreaticobiliary system: the common bile duct (CBD); the right intrahepatic duct (RIHD); the left intrahepatic duct (LIHD); cystic duct insertion; and main pancreatic duct (MPD) in the proximal, middle, and distal segments. For each segment, ductal visualization was graded on a 5-point Likert-type scale (1 = ductal structure not visible, 2 = ductal structure vaguely identified, 3 = ductal structure partially visible, 4 = most of the ductal structure visible with some blurring, 5 = entire ductal structure visible with excellent details). An average score from the 2 readers was used to determine the adequate visualization of the ductal system. Adequate visualization of the entire biliary system was determined if CBD, RIHD, LIHD, and cystic duct visualization all achieved an average score of 3 or higher. Adequate visualization of the entire pancreatic duct was determined if the proximal, middle, and distal pancreatic duct all achieved an average score of 3 or higher.

Evaluation of Duct-Related Pathology

The 2 radiologists independently evaluated pancreatic duct morphology and duct-related pathologies. The presence of anatomical anomalies/variants of pancreatic ducts, including pancreatic divisum,[19] annular pancreas,[20] anomalous pancreaticobiliary ductal union (APBDU),[21] bifid MPD configuration, ansa pancreatica, and ductal loops,[22,23] was determined on a 5-point scale and recorded (1 = definitely absent, 2 = probably absent, 3 = indeterminate, 4 = probably present; 5 = definitely present). The presence of focal or long-segment pancreatic duct stenosis, which was considered characteristic of autoimmune pancreatitis,[24,25] was evaluated in the same manner. The presence of abnormal branches of pancreatic duct and the number of abnormal branches were recorded.[26] In patients with cystic pancreatic lesions, the presence of lesion communication with MPD was evaluated.[27,28] When multiple cystic lesions were present, lesion-MPD communication was only evaluated for the largest lesion.

The reference standard of duct-related pathologies was based on the final clinical diagnosis combining evidence from radiological and endoscopic studies, surgical pathologies, and treatment response (Fig. 1).

Statistical Analysis

The Friedman test was used to compare the acquisition time, artifact, background suppression, and image quality of the biliary and pancreatic ducts among conventional NT, CS-NT, and CS-BH MRCP protocols, followed by post hoc analysis.

Interobserver agreement of the qualitative results was determined by calculating κ values (0.21–0.40, fair agreement; 0.41–0.60, moderate; 0.61–0.80, good; 0.81–1.00, excellent agreement). Receiver operating characteristic (ROC) curve analysis of the duct-related pathologies was performed, and the area under the ROC curves (A_z) was

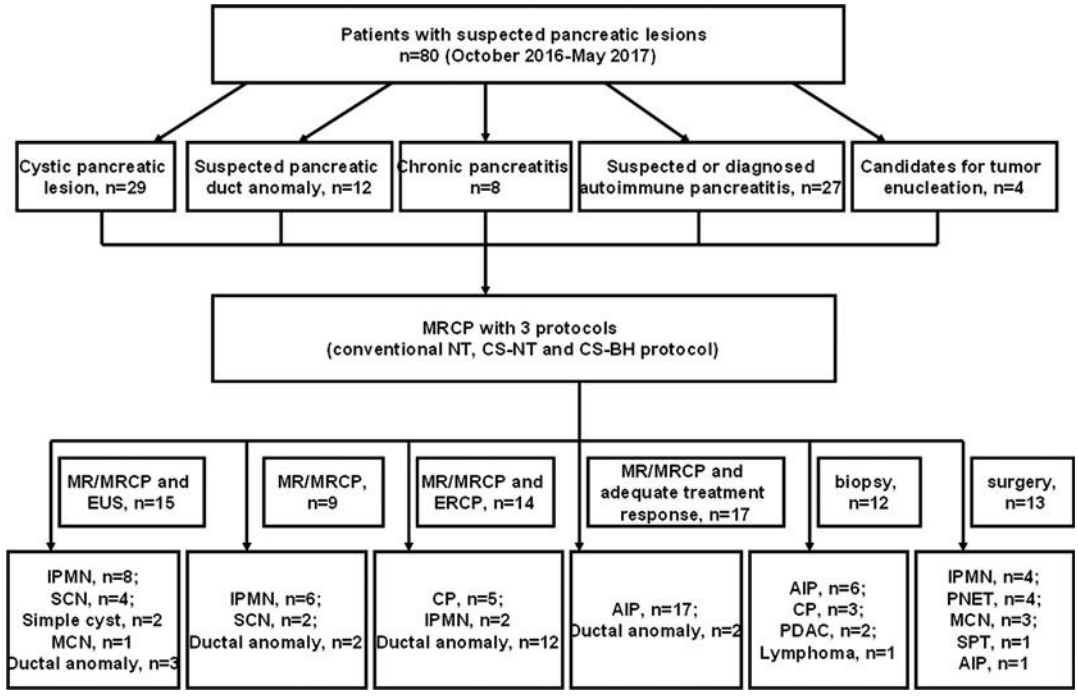

FIGURE 1. Flowchart. IPMN, intraductal papillary mucinous neoplasm; MCN, mucinous cystic neoplasm; SCN, serous cystadenoma; PDAC, pancreatic ductal adenocarcinoma; AIP, autoimmune pancreatitis; PNET, pancreatic neuroendocrine tumor; SPT, solid pseudopapillary tumor.

calculated using the nonparametric trapezoidal rule and compared to determine the diagnostic performance of the MRCP protocols.[29] Mean sensitivity, specificity, and accuracy were also calculated, taking rating scales of 4 or greater as positive. Statistical analysis was performed using SPSS 17.0 software (IBM Corp, Armonk, NY). A 2-sided *P* value of less than 0.05 after false discovery rate correction for multiple testing was considered to indicate a significant difference.

RESULTS

The final diagnosis of the patient cohort was intraductal papillary mucinous neoplasm in 20 (branch-duct type, n = 14; main-duct type and mixed type, n = 6), mucinous cystic neoplasm in 4, serous cystadenoma in 6, simple pancreatic cyst in 2, chronic pancreatitis in 8, autoimmune pancreatitis in 24, pancreatic ductal adenocarcinoma in 2, pancreatic neuroendocrine tumors in 4, solid pseudopapillary neoplasm in 1, and pancreatic lymphoma in 1. Pancreatic duct anomaly/variants were found in 19 patients, including pancreatic divisum in 9, APBDU in 1, bifid MPD configuration in 6, and ansa pancreatica in 3 (Fig. 1). Eleven of 19 patients who were found to have pancreatic duct anomalies/variants were incidental findings coexisting with other pathological conditions.

Acquisition Time and Image Quality

The 3D MRCP examinations with all 3 protocols were successfully performed in all patients. The acquisition time of CS-BH MRCP was 17 seconds, and the average acquisition time of CS-NT MRCP was 134.1 ± 33.5 seconds (range, 89–204 seconds), both significantly shorter compared with conventional NT MRCP (364.7 ± 78.4 seconds; range, 274–587 seconds; for both, $P < 0.01$).

Image quality and duct visualization of the 3 protocols are shown in Table 1. Overall image quality degradation by artifacts was most severe with conventional NT MRCP. The CS-BH protocol showed significantly less artifacts compared with conventional NT and CS-NT MRCP (both $P < 0.001$). The incidence of severe artifacts was 3.8% with the CS-BH protocol, 10.6% with CS-NT, and 16.3% with the conventional NT protocol. Similar background signal suppression was achieved with conventional NT and CS-NT MRCP (4.26 ± 0.79 and 4.32 ± 0.59, respectively), both of which were significantly better compared with the CS-BH protocol (3.83 ± 0. 55; both $P < 0.001$).

The visualization of bile ducts was generally comparable with the 3 protocols. There was no significant difference concerning visualization of CBD, RIHD, LIHD, and cystic duct between any 2 MRCP protocols. Adequate visualization of the entire biliary tree was achieved in 91.3% (73/80) of the patients with CS-NT MRCP, 85.0% (68/80) with the conventional NT MRCP, and 93.8% (75/80) with CS-BH MRCP.

Conventional NT and CS-NT MRCP depicted the pancreatic duct significantly better compared with CS-BH MRCP. Visualization of proximal, middle, and distal MPD was comparable with conventional NT and CS-NT MRCP ($P = 0.40$, 0.43, and 0.68, respectively), both of which were significantly better compared with CS-BH MRCP ($P < 0.001$ to $P = 0.03$). After multiple testing, the difference between conventional NT and CS-BH MRCP in proximal MPD became insignificant, and for all the other comparisons, the differences remain significant. Adequate visualization of the entire pancreatic duct was achieved in 90.0% (72/80) of patients with CS-NT MRCP, 82.5% (66/80) with the conventional NT MRCP, and 76.3% (61/80) with CS-BH MRCP.

In 8 patients, visualization of the pancreatic duct was compromised with CS-NT MRCP, and image quality degradation involved 5 proximal segments, 6 middle segments, and 8 distal segments. With the addition of CS-BH MRCP, visualization of these blurred segments was improved, and adequate visualization of the entire pancreatic duct was achieved in 6 patients.

Interobserver Agreement

Interobserver agreement of the qualitative results is summarized in Table 2. Good to excellent agreement was shown for conventional NT MRCP (weighted κ = 0.64–0.83), CS-NT MRCP (weighted κ = 0.67–0.89), and CS-BH MRCP (weighted κ = 0.62–0.85).

TABLE 1. Image Quality Scores for the Pancreaticobiliary System

	Conventional NT MRCP	CS-NT MRCP	CS-BH MRCP	*P*	*P**	*P*†
Artifacts	3.31 ± 0.98 (1.5–5)	3.56 ± 0.83 (2.5–5)	3.91 ± 0.29 (4–5)	0.004‡	<0.001‡	<0.001‡
Background suppression	4.26 ± 0.79 (2–5)	4.32 ± 0.59 (2–5)	3.83 ± 0.55 (3–5)	0.51	<0.001‡	<0.001‡
Duct visualization						
CBD	4.64 ± 0.68 (2–5)	4.75 ± 0.48 (3–5)	4.81 ± 0.36 (4–5)	0.18	0.07	0.15
RIHD	4.44 ± 0.98 (1.5–5)	4.51 ± 0.77 (3–5)	4.69 ± 0.47 (4–5)	0.57	0.08	0.16
LIHD	4.27 ± 1.02 (1–5)	4.40 ± 0.85 (2–5)	4.64 ± 0.51 (3.5–5)	0.49	0.06	0.17
Cystic duct	4.15 ± 1.19 (1–5)	4.22 ± 099 (1.5–5)	4.25 ± 0.84 (2.5–5)	0.47	0.61	0.99
Proximal MPD	4.14 ± 1.01 (2.5–5)	4.29 ± 1.05 (2.5–5)	3.71 ± 1.27 (1.5–5)	0.40	0.03	0.002‡
Middle MPD	4.09 ± 1.05 (2–5)	4.18 ± 1.02 (2–5)	3.27 ± 0.98 (1.5–5)	0.43	0.001‡	<0.001‡
Distal MPD	4.01 ± 1.03 (2–5)	3.96 ± 1.18 (2–5)	3.42 ± 1.24 (1–5)	0.68	0.003‡	0.01‡

Values are presented as mean ± standard deviation (range).

P value is for comparison between conventional NT and CS-NT protocols: **P* value is for comparison between conventional NT and CS-BH protocols. †*P* value is for comparison between CS-NT and CS-BH protocols.

‡The *P* values indicate significant difference after adjustment for multiple testing.

NT indicates navigator-triggered; MRCP, magnetic resonance cholangiopancreatography; CS, compressed-sensing; BH, breath-hold; CBD, common bile duct; RIHD, right intrahepatic duct; LIHD, left intrahepatic duct; MPD, main pancreatic duct.

Duct-Related Pathology and ROC Curves

For the duct-related pathologies, the mean A_z value and mean sensitivity and specificity for the 3 MRCP protocols are listed in Table 3. For detecting ductal anomalies, the mean A_z values for CS-NT MRCP and conventional NT-MRCP were 0.943 and 0.908, both being significantly higher compared with that for CS-BH MRCP (0.756; for both, $P < 0.05$). Of note, although the specificity was high for all 3 protocols, the sensitivity was poor for the CS-BH protocol (31.6%, compared with 78.9% for the CS-NT protocol and 63.2% for the conventional NT protocol), revealing a higher chance for ductal anomalies to be missed with CS-BH MRCP (Figs. 2 and 4). For identification of long-segment pancreatic duct stenosis, which is a characteristic finding for inflammatory pancreatic masses, the mean A_z values were highest for CS-NT MRCP (0.983), compared with conventional NT MRCP (0.901) and CS-BH MRCP (0.811). The difference between CS-NT and CS-BH MRCP was significant ($P < 0.05$) (Fig. 3). For detecting abnormal branch ducts, CS-NT MRCP and conventional NT MRCP both achieved high diagnostic accuracy, with mean A_z values of 0.967 and 0.956, respectively, whereas the diagnostic performance was poorer with CS-BH MRCP (mean A_z value, 0.787). The mean A_z values of CS-NT and conventional NT MRCP were both significantly higher than CS-BH MRCP (both $P < 0.05$). The sensitivity of CS-BH MRCP was decreased (56.5%), compared with CS-NT MRCP (78.3%) and conventional NT MRCP (73.9%). The median number of abnormal branch ducts detected was 3 (range, 1–12), 4.5 (range, 1–11), and 1 (range, 0–5) with conventional NT, CS-NT, and CS-BH MRCP, respectively (Fig. 4). All 3 protocols demonstrate high diagnostic accuracy for detecting pancreatic cystic lesions. However, concerning observation of the communication between cystic lesion and pancreatic duct, CS-NT MRCP was significantly better compared with the other 2 protocols. The mean A_z value was 0.982 for CS-NT MRCP, which was significantly higher compared with that for conventional NT MRCP (0.851) and CS-BH MRCP (0.839; both, $P < 0.05$).

DISCUSSION

In this clinical study, CS accelerated 3D MRCP was successfully obtained both in BH mode and in NT mode. Acquisition time was significantly shortened compared with conventional NT MRCP. The scale of time reduction was 2.7-fold in the CS-NT protocol and 21.5-fold in

TABLE 2. Reader Agreement of Qualitative Image Evaluation

	Conventional NT MRCP	CS-NT MRCP	CS-BH MRCP
Artifacts	0.83 (0.76–0.89)	0.81 (0.75–0.87)	0.78 (0.72–0.83)
Background suppression	0.67 (0.57–0.76)	0.72 (0.63–0.80)	0.66 (0.42, 0.78)
Duct visualization			
CBD	0.79 (0.73–0.85)	0.89 (0.84–0.93)	0.85 (0.80–0.90)
RIHD	0.69 (0.59–0.76)	0.78 (0.72–0.83)	0.79 (0.72–0.85)
LIHD	0.73 (0.67–0.79)	0.80 (0.74–0.85)	0.80 (0.75–0.86)
Cystic duct	0.64 (0.52–0.75)	0.67 (0.56–0.77)	0.62 (0.50–0.73)
Proximal MPD	0.78 (0.72–0.83)	0.77 (0.70–0.82)	0.73 (0.67–0.79)
Middle MPD	0.74 (0.65–0.82)	0.72 (0.63–0.79)	0.69 (0.59–0.76)
Distal MPD	0.66 (0.42–0.78)	0.67 (0.56–0.77)	0.64 (0.52–0.75)

Numbers in parenthesis are 95% confidence interval.

NT indicates navigator-triggered; MRCP, magnetic resonance cholangiopancreatography; CS, compressed-sensing; BH, breath-hold; CBD, common bile duct; RIHD, right intrahepatic duct; LIHD, left intrahepatic duct; MPD, main pancreatic duct.

TABLE 3. Mean A_z Value and Diagnostic Accuracy of Conventional NT MRCP, CS-NT MRCP, and CS-BH MRCP for Detecting Duct-Related Pathologies

	Conventional NT MRCP			CS-NT MRCP			CS-BH MRCP		
	A_z value	Sensitivity (%)	Specificity (%)	A_z Value	Sensitivity (%)	Specificity (%)	A_z Value	Sensitivity (%)	Specificity (%)
Ductal anomaly	0.908	63.2 (12/19)	91.8 (56/61)	0.943	78.9 (15/19)	93.4 (57/61)	0.756	31.6 (6/19)	90.2 (55/61)
Long segment MPD stenosis	0.901	72.0 (18/25)	85.5 (47/55)	0.983	88.0 (22/25)	96.4 (53/55)	0.811	76.0 (19/25)	65.5 (36/55)
Abnormal branch ducts	0.956	73.9 (17/23)	94.7 (54/57)	0.967	78.3 (18/23)	96.5 (55/57)	0.787	56.5 (13/23)	96.5 (55/57)
Cystic lesion	NA	90.1 (29/32)	97.9 (47/48)	NA	100.0 (32/32)	95.8 (46/48)	NA	96.9 (31/32)	93.8 (45/48)
Cystic lesion-MPD communication	0.851	58.8 (10/17)	93.3 (14/15)	0.982	82.4 (14/17)	100.0 (15/15)	0.839	52.9 (9/17)	93.3 (14/15)

Values in the parentheses indicate number of patients with positive findings divided by the total number of patients.

NT indicates navigator-triggered; MRCP, magnetic resonance cholangiopancreatography; CS, compressed-sensing; BH, breath-hold; MPD, main pancreatic duct; NA, not applicable.

the CS-BH protocol on average. The overall image quality and the visualization of the bile duct structures were comparable or superior compared with the conventional NT protocol, which is in accordance with previous studies.[15–17] Compared with NT protocols, artifacts were significantly less severe with the CS-BH protocol. Only 3.8% patients had severe artifacts with the CS-BH protocol, whereas in the same study population, the prevalence of severe artifacts was 10.6% to 16.3% with NT protocols. It has been demonstrated that longer acquisition time causes a higher prevalence of diaphragmatic drifting, thus degrading image quality.[3] Therefore, the more respiratory circles are needed for data sampling, the higher the chance of artifacts. The acquisition time of CS-NT MRCP is shorter than that of conventional NT MRCP, and

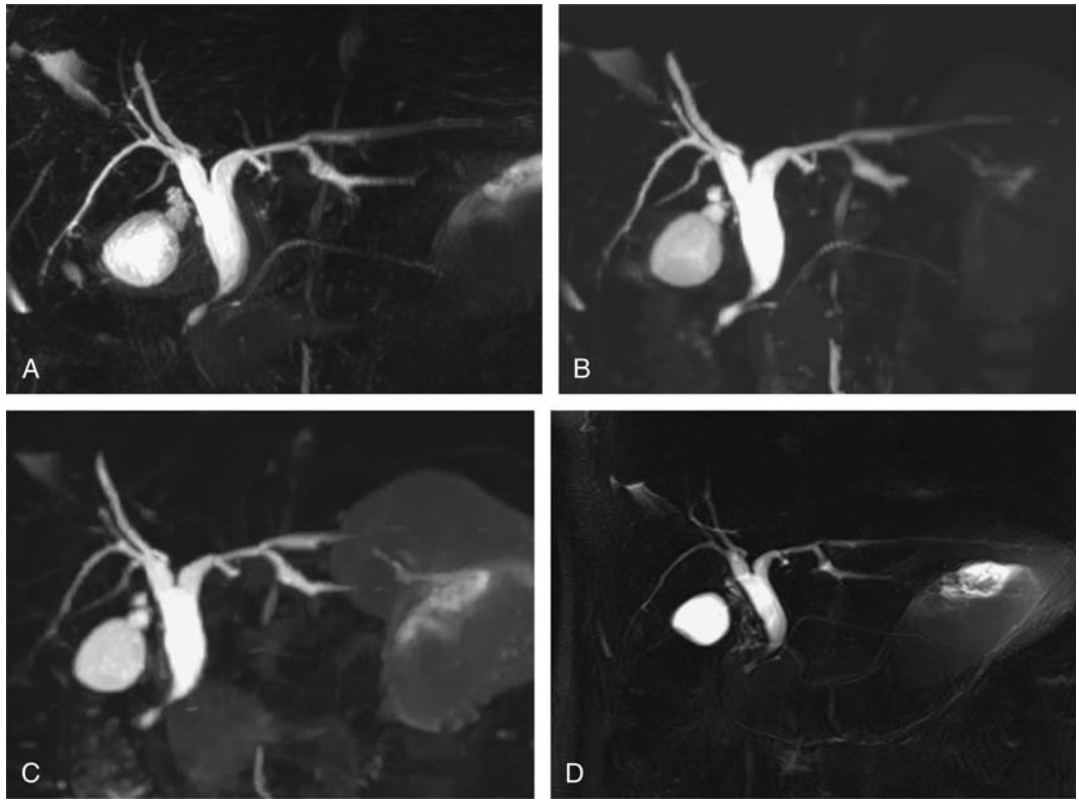

FIGURE 2. A 39-year-old woman with 3 months' onset of mild epigastric pain. Abdominal ultrasound and contrast-enhanced CT revealed CBD dilation without obvious mass lesion. Conventional NT 3D MRCP (A) had good image quality and revealed the common channel between distal CBD and pancreatic duct, consistent with type A APBDU. CS-NT MRCP (B) showed good image quality as well, and the background suppression was better. The entire pancreatic duct and the abnormal pancreaticobiliary union were depicted clearly. CS-BH MRCP (C) depicted the biliary tree with good image quality. However, the MPD was only partially visible with low contrast, and the anomalous pancreaticobiliary connection was unseen. The background signal suppression was suboptimal. Single-shot turbo spin echo 2D MRCP (D) is shown as reference. The acquisition time of conventional NT, CS-NT, and CS-BH MRCP was 385, 193, and 17 seconds, respectively.

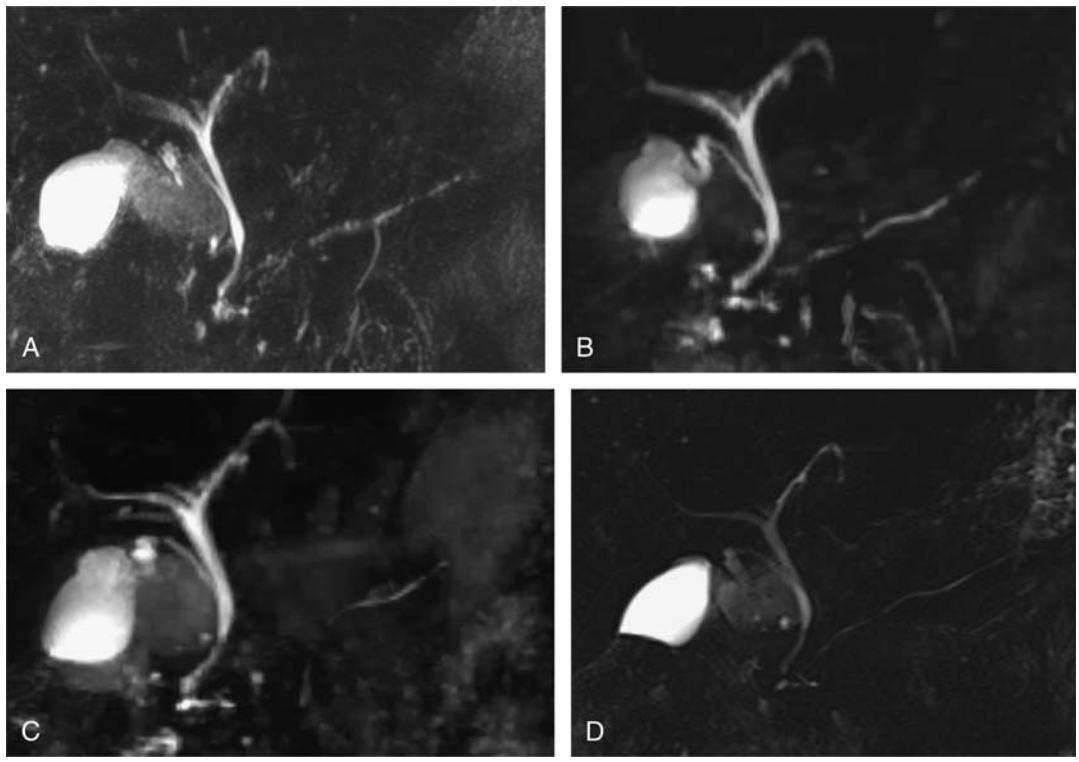

FIGURE 3. A 57-year-old man with autoimmune pancreatitis. Conventional NT 3D MRCP (A) had mild respiratory movement artifacts. The MPD appeared irregular, with several long-segment stenosis. However, the margin of MPD was blurred, and the background signal suppression was suboptimal. CS-NT MRCP (B) showed better overall image quality and background suppression, and the entire MPD is depicted clearly, revealing the abnormal ductal morphology. CS-BH MRCP (C) depicted the biliary tree with good image quality. The MPD was almost undetectable in the pancreatic head and body segment, and the diagnostic information was lost. Besides, background suppression was suboptimal with CS-BH MRCP. Single-shot turbo spin echo 2D MRCP (D) was shown as reference. The acquisition time of conventional NT, CS-NT, and CS-BH MRCP was 416, 202, and 17 seconds, respectively.

the artifacts are less pronounced. The acquisition time of our CS-BH protocol was 17 seconds, which was well tolerated by most patients, with the least respiratory artifacts.

Despite of the advantages of CS-BH MRCP discussed above, we found that CS-BH MRCP seems to be less accurate concerning visualization of the more delicate pancreatic duct structure. In our study, adequate visualization of the entire pancreatic duct was achieved in only 76.3% patients with the CS-BH protocol, compared with 90.0% with the CS-NT protocol. According to our observation, suboptimal pancreatic duct visualization was seldom caused by artifact-related image blurring, rather by weak signal intensity of the thin pancreatic duct and less well background signal suppression with CS-BH MRCP. Yoon et al[17] have also reported that CS MRCP had lower background suppression compared with conventional MRCP. In their study, a direct comparison of conventional NT, CS-NT, and CS-BH protocol was performed in 28 patients. Similar to our results, CS-NT protocol achieved the highest image quality of the pancreatic duct. However, the difference between the CS-NT and CS-BH protocols was insignificant. This was probably due to the limited number of cases and the fact that the pancreatic duct was grossly evaluated without specific segmental analysis. Inadequate duct visualization involving part of the pancreatic duct could be overlooked in this manner. In our study focusing on pancreatic diseases, several challenges for CS-BH MRCP was identified. Besides compromised visualization of the entire pancreatic duct encompassing the proximal, middle, and distal segments, subtle pancreatic duct anomalies/variants were also less obvious and sometimes missed, and the number of abnormal side branches detected was lower. These facts all suggest that CS-BH MRCP, although less prone to artifacts, might not be the optimal protocol for evaluating pancreatic diseases. The more direct evidences were provided by the diagnostic performance of several duct-related pathologies.

In this study, 19 of 80 patients had the diagnosis of pancreatic duct anomaly/variants. Developmental anomalies of the pancreatic duct system could be asymptomatic, but they are more frequently seen in patients with idiopathic or recurrent pancreatitis.[30] The definite diagnosis used to be made by endoscopic retrograde pancreatography, MRCP also demonstrated high sensitivity and specificity for the diagnosis.[1,31] The diagnosis with MRCP relies on a close inspection of the pancreatic duct drainage and connection between the dorsal and ventral duct.[19] In our study, the sensitivity of diagnosing duct anomalies was quite low with CS-BH MRCP (31.6%), whereas CS-NT MRCP was able to detect 78.9% of the anomalies. The "duct-penetrating sign," described as a long-segment stenotic, but not obstructed pancreatic duct within a mass-like pancreatic lesion, has been considered a useful sign for differentiating inflammatory pancreatic mass from pancreatic carcinomas.[25] The presence of multiple, long-segment stenoses of pancreatic duct, without dilation, was considered characteristic for focal autoimmune pancreatitis.[24] The sensitivity and specificity of diagnosing long-segment duct stenosis were less satisfactory with CS-BH MRCP, compared with CS-NT MRCP. The number and morphology of abnormal branch ducts provide useful diagnostic information for chronic pancreatitis.[26,32] The lowest number of abnormal branch ducts was detected by CS-BH MRCP, and the highest, by CS-NT MRCP. Direct communication between a cystic lesion and pancreatic duct is pathognomonic for intraductal papillary mucinous neoplasms. Magnetic resonance cholangiopancreatography is considered superior to computed tomography for detecting the ductal connection,[33] and 3D MRCP is preferred to 2D

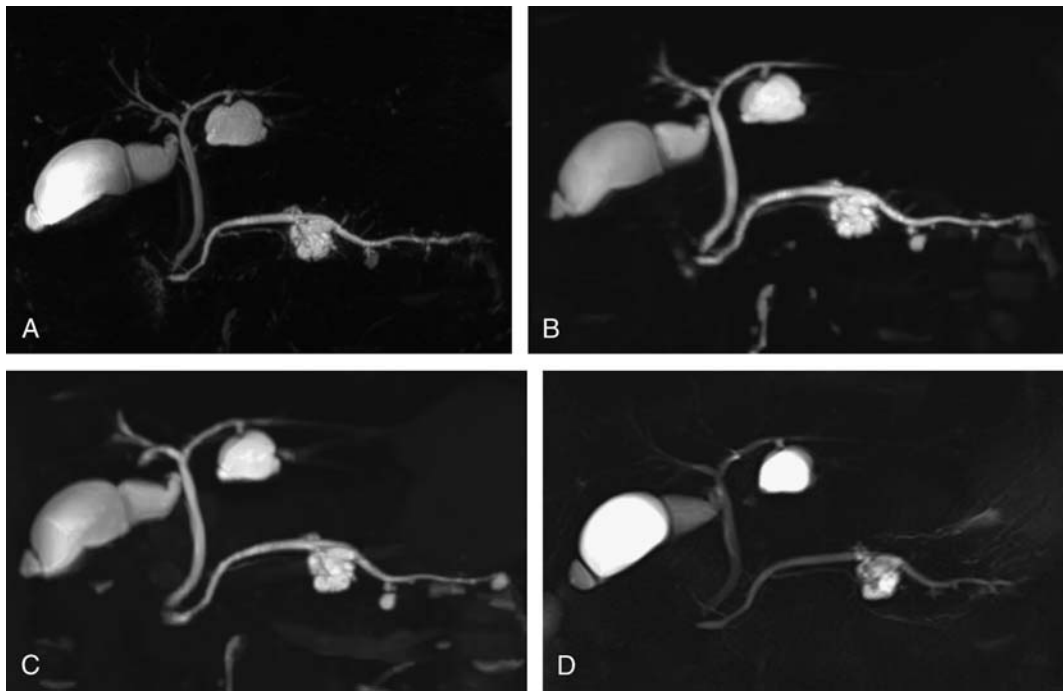

FIGURE 4. A 67-year-old man with incidental pancreatic cystic lesion detected by abdominal ultrasound. The final diagnosis was multiple branch-duct IPMN. Conventional NT 3D MRCP (A), CS-NT MRCP (B), and CS-BH MRCP (C) all had good overall image quality, and the largest cystic lesion in the pancreatic body was demonstrated with clear details. Communication of the cystic lesion to pancreatic duct was shown. The bifid configuration of the MPD, however, was invisible with CS-BH MRCP. The number of abnormal branch ducts demonstrated by CS-BH MRCP was also lower compared to the other 2 acquisition methods. Single-shot turbo spin echo 2D MRCP (D) is shown as reference. The acquisition time of conventional NT, CS-NT, and CS-BH MRCP was 340, 144, and 17 seconds, respectively.

MRCP for surgical planning.[27] Among the 3D MRCP protocols under evaluation, CS-NT MRCP yielded the highest diagnostic accuracy for communication between cystic lesion and pancreatic duct, which is significantly better than the other 2 protocols.

Through diagnostic performance analysis of common duct-related pathologies, we have demonstrated that CS-NT MRCP is the preferred protocol for imaging patients with suspected pancreatic diseases, owing to the higher overall image quality and superior diagnostic performance for pancreatic duct–related pathologies. Nevertheless, in patients with drifting respiratory patterns or in whom a shorter imaging time is desired, CS-BH MRCP could be a useful supplemental technique. It should be kept in mind, however, that the pancreatic duct–related pathologies need to be interpreted with caution when the CS-BH protocol is applied because the pathological conditions might be overestimated (such as duct stenosis) or underestimated (such as branch duct dilation) with CS-BH MRCP. Information from the other sequences of pancreatic MR and the clinical findings of the individual patient may aid for a more accurate diagnosis.

Our study has several limitations. First, this prospective study was carried out in a highly specialized pancreatic disease center, and institutional bias was unavoidable. Second, the reference standard was based on the final results of multidisciplinary workup, including endoscopic and surgical operations, and not all the patients had histological confirmation of the diagnosis. Third, although we tried to keep the scanning parameters identical, because of the current restrictions of the prototype CS approach, there are slight differences in the acquisition parameters between the conventional and CS MRCP. Last, but not the least, the reconstruction process of CS BH MRCP was not fully optimized. Optimization of the algorithm parameters of the iterative reconstruction might enhance the performance of the BH protocol.[34] Reconstruction time, however, might have to be further elongated, which might not be suitable for clinical practices. Further development, for example, applying graphics processing unit in reconstruction, might overcome this challenge.

In conclusion, CS-MRCP provides comparable or superior image quality than conventional MRCP and reduces scanning time. Compressed-sensing-NT MRCP demonstrated superior diagnostic accuracy for duct-related pathologies, and is preferred for patients with suspected pancreatic diseases.

ACKNOWLEDGMENT

The authors acknowledge Guobin Li for his work on the pulse sequence prototype and Christoph Forman, Jens Wetzl, and Michael O. Zenge for their work on the image reconstruction framework. The authors also acknowledge Prof. Bernd Hamm from the Department of Radiology, Charité–Universitätsmedizin Berlin, for his kind help during the manuscript preparation.

REFERENCES

1. Barish MA, Yucel EK, Ferrucci JT. Magnetic resonance cholangiopancreatography. *N Engl J Med*. 1999;341:258–264.
2. Irie H, Honda H, Tajima T, et al. Optimal MR cholangiopancreatographic sequence and its clinical application. *Radiology*. 1998;206:379–387.
3. Taylor AC, Little AF, Hennessy OF, et al. Prospective assessment of magnetic resonance cholangiopancreatography for noninvasive imaging of the biliary tree. *Gastrointest Endosc*. 2002;55:17–22.
4. Calvo MM, Bujanda L, Calderón A, et al. Comparison between magnetic resonance cholangiopancreatography and ERCP for evaluation of the pancreatic duct. *Am J Gastroenterol*. 2002;97:347–353.
5. Glockner JF, Saranathan M, Bayram E, et al. Breath-held MR cholangiopancreatography (MRCP) using a 3D Dixon fat-water separated balanced steady state free precession sequence. *Magn Reson Imaging*. 2013;31:1263–1270.
6. Asbach P, Dewey M, Klessen C, et al. Respiratory-triggered MRCP applying parallel acquisition techniques. *J Magn Reson Imaging*. 2006;24:1095–1100.

7. Zhang J, Israel GM, Hecht EM, et al. Isotropic 3D T2-weighted MR cholangiopancreatography with parallel imaging: feasibility study. *AJR Am J Roentgenol*. 2006;187:1564–1570.
8. Itatani R, Namimoto T, Takaoka H, et al. Clinical impact of 3-dimensional balanced turbo-field-echo magnetic resonance cholangiopancreatography at 3 T: prospective intraindividual comparison with 3-dimensional turbo-spin-echo magnetic resonance cholangiopancreatography. *J Comput Assist Tomogr*. 2015;39:19–24.
9. Fushimi Y, Fujimoto K, Okada T, et al. Compressed sensing 3-dimensional time-of-flight magnetic resonance angiography for cerebral aneurysms: optimization and evaluation. *Invest Radiol*. 2016;51:228–235.
10. Runge VM, Richter JK, Heverhagen JT. Speed in clinical magnetic resonance. *Invest Radiol*. 2017;52:1–17.
11. Chandarana H, Feng L, Ream J, et al. Respiratory motion-resolved compressed sensing reconstruction of free-breathing radial acquisition for dynamic liver magnetic resonance imaging. *Invest Radiol*. 2015;50:749–756.
12. Benkert T, Block KT, Heller S, et al. Comprehensive dynamic contrast-enhanced 3D magnetic resonance imaging of the breast with fat/water separation and high spatiotemporal resolution using radial sampling, compressed sensing, and parallel imaging. *Invest Radiol*. 2017;52:583–589.
13. Yang AC, Kretzler M, Sudarski S, et al. Sparse reconstruction techniques in magnetic resonance imaging: methods, applications, and challenges to clinical adoption. *Invest Radiol*. 2016;51:349–364.
14. Yamamoto T, Fujimoto K, Okada T, et al. Time-of-flight magnetic resonance angiography with sparse undersampling and iterative reconstruction: comparison with conventional parallel imaging for accelerated imaging. *Invest Radiol*. 2016; 51:372–378.
15. Chandarana H, Doshi AM, Shanbhogue A, et al. Three-dimensional MR cholangiopancreatography in a breath hold with sparsity-based reconstruction of highly undersampled data. *Radiology*. 2016;280:585–594.
16. Seo N, Park MS, Han K, et al. Feasibility of 3D navigator-triggered magnetic resonance cholangiopancreatography with combined parallel imaging and compressed sensing reconstruction at 3 T [published online ahead of print March 11, 2017]. *J Magn Reson Imaging*. 2017. doi: 10.1002/jmri.25672.
17. Yoon JH, Lee SM, Kang HJ, et al. Clinical feasibility of 3-dimensional magnetic resonance cholangiopancreatography using compressed sensing: comparison of image quality and diagnostic performance. *Invest Radiol*. 2017;52:612–619.
18. Otazo R, Kim D, Axel L, et al. Combination of compressed sensing and parallel imaging for highly accelerated first-pass cardiac perfusion MRI. *Magn Reson Med*. 2010;64:767–776.
19. Boninsegna E, Manfredi R, Ventriglia A, et al. Santorinicele: secretin-enhanced magnetic resonance cholangiopancreatography findings before and after minor papilla sphincterotomy. *Eur Radiol*. 2015;25:2437–2444.
20. Yu J, Turner MA, Fulcher AS, et al. Congenital anomalies and normal variants of the pancreaticobiliary tract and the pancreas in adults: part 2, pancreatic duct and pancreas. *AJR Am J Roentgenol*. 2006;187:1544–1553.
21. Kim MJ, Han SJ, Yoon CS, et al. Using MR cholangiopancreatography to reveal anomalous pancreaticobiliary ductal union in infants and children with choledochal cysts. *AJR Am J Roentgenol*. 2002;179:209–214.
22. Sigfússon BF, Wehlin L, Lindström CG. Variants of pancreatic duct system of importance in endoscopic retrograde cholangiopancreatography. Observations on autopsy specimens. *Acta Radiol Diagn (Stockh)*. 1983;24:113–128.
23. Tanaka T, Ichiba Y, Miura Y, et al. Variations of the pancreatic ducts as a cause of chronic alcoholic pancreatitis; ansa pancreatica. *Am J Gastroenterol*. 1992; 87:806.
24. Negrelli R, Manfredi R, Pedrinolla B, et al. Pancreatic duct abnormalities in focal autoimmune pancreatitis: MR/MRCP imaging findings. *Eur Radiol*. 2015;25: 359–367.
25. Ichikawa T, Sou H, Araki T, et al. Duct-penetrating sign at MRCP: usefulness for differentiating inflammatory pancreatic mass from pancreatic carcinomas. *Radiology*. 2001;221:107–116.
26. Sarner M, Cotton PB. Classification of pancreatitis. *Gut*. 1984;25:756–759.
27. Yoon LS, Catalano OA, Fritz S, et al. Another dimension in magnetic resonance cholangiopancreatography: comparison of 2- and 3-dimensional magnetic resonance cholangiopancreatography for the evaluation of intraductal papillary mucinous neoplasm of the pancreas. *J Comput Assist Tomogr*. 2009;33:363–368.
28. Sahani DV, Kadavigere R, Blake M, et al. Intraductal papillary mucinous neoplasm of pancreas: multi-detector row CT with 2D curved reformations—correlation with MRCP. *Radiology*. 2006;238:560–569.
29. Hanley JA, McNeil BJ. The meaning and use of the area under a receiver operating characteristic (ROC) curve. *Radiology*. 1982;143:29–36.
30. Mortelé KJ, Rocha TC, Streeter JL, et al. Multimodality imaging of pancreatic and biliary congenital anomalies. *Radiographics*. 2006;26:715–731.
31. Manfredi R, Costamagna G, Brizi MG, et al. Pancreas divisum and "santorinicele": diagnosis with dynamic MR cholangiopancreatography with secretin stimulation. *Radiology*. 2000;217:403–408.
32. Forsmark CE. The diagnosis of chronic pancreatitis. *Gastrointest Endosc*. 2000; 52:293–298.
33. Waters JA, Schmidt CM, Pinchot JW, et al. CT vs MRCP: optimal classification of IPMN type and extent. *J Gastrointest Surg*. 2008;12:101–109.
34. Feng L, Grimm R, Block KT, et al. Golden-angle radial sparse parallel MRI: combination of compressed sensing, parallel imaging, and golden-angle radial sampling for fast and flexible dynamic volumetric MRI. *Magn Reson Med*. 2014; 72:707–717.